Effect of Endplate Shape on Performance and Stability of Wings-in Ground (WIG) Craft

Kyoungwoo Park, Chol Ho Hong, Kwang Soo Kim and Juhee Lee

Abstract—Numerical analysis for the aerodynamic characteristics of the WIG (wing-in ground effect) craft with highly cambered and aspect ratio of one is performed to predict the ground effect for the case of with- and without- lower-extension endplate. The analysis is included varying angles of attack from 0 to10 deg. and ground clearances from 5% of chord to 50%. Due to the ground effect, the lift by rising in pressure on the lower surface is increased and the influence of wing-tip vortices is decreased. These two significant effects improve the lift-drag ratio. On the other hand, the endplate prevents the high-pressure air escaping from the air cushion at the wing tip and causes to increase the lift and lift-drag ratio further. It is found from the visualization of computation results that two wing-tip vortices are generated from each surface of the wing tip and their strength are weak and diminished rapidly. Irodov's criteria are also evaluated to investigate the static height stability. The comparison of Irodov's criteria shows that the endplate improves the deviation of the static height stability with respect to pitch angles and heights. As the results, the endplate can improve the aerodynamic characteristics and static height stability of wings in ground effect, simultaneously.

Keywords— WIG craft, Endplate, Ground Effect, Aerodynamics, CFD, Lift-drag ratio, Static height stability.

I. INTRODUCTION

ACCORDING to the globalization and information technology of the industries, the transportation has become a center of key industries. The von Karman-Gabriell's diagram [1] depicts the efficiency of various transportations. A remarkable thing is the triangular area at the center of the technology line where no conventional means of transportation appears. The WIG (wing-in-ground effect) craft, a flying ship cruising with the speed of 100 to 400 km/h and the lift-to-drag of 15 to 30, can fill the speed and efficiency gap between marines and air transports. In general, the lift and drag forces of an airfoil will change considerably near ground. These phenomena have been observed by many researches [2]-[5]. According to their results, the ground exerts a great influence (suction and stagnation) on pressure distribution along the wing

Kyoungwoo Park is with the Department of Mechanical Engineering, Hoseo University, Asan, Choongnam 336-795, Korea (phone: +82-41-540-5804; fax: +82-41-540-5808; e-mail: kpark@ hoseo.edu).
Chol Ho Hong is with the Department of System Control Engineering, Hoseo University, Asan, Choongnam 336-795, Korea (phone: +82-41-540-5671; fax: +82-41-540-5678; e-mail: chhong@ hoseo.edu).
Juhee Lee is with the Department of Mechatronics, Hoseo University, Asan, Choongnam 336-795, Korea (phone: +82-41-540-9669; fax: +82-41-540-5246; e-mail: juheelee@ hoseo.edu).

surface. Flows coming to the lower surface gradually decrease the magnitude of the speed and cause to change the dynamic pressure to static pressure. Pressure distributions on the lower surface become constant somewhat and the strength of the pressure increase as the ground proximity. As the suction on the upper surface also shrinks or extends according to the wing profile, the pressure distributions change. In general, the pressure rise is considerably high and the resultant forces of the pressure on both surfaces lead increasing in the lift forces when the wing is under the ground effect. The center of the pitching moment moves to the mid span where is behind the center of gravity because of constant pressure distributions. For the finite wing in three-dimensional flow, the induced drag decreases because the influence of the wing tip vortex decreases while the strength of the wing-tip vortex is increase. The endplate prevent the flow exiting through the wing tip instead of the small gap at the trailing edge and increase the ground effect exerting on the wing surface. The theoretical investment of the ground effect was performed to determine the conditions in taking off and landing of an airplane with Prandtl's wing theory [2]. He utilized the principle of reflection and replaced the surface of the ground by the second wing at the same distance but on the opposite side. The reduction in induced drag of a mono plane and multi plane in ground effect was estimated in terms of the ground influence coefficient, aspect ratio, and lift coefficient. The comparison of theoretical and experiment results were in good agreement. Fink et al. [3] performed a series of wind- tunnel investigations to determine the ground effect on the aerodynamic characteristics of thick highly cambered wings with various aspect ratios. They used the two wings on opposite side of the imaginary ground. All wings in the experiments increase the lift slope and reduce the induced drag which results in the increase of lift-drag ratio. They predicted an increase in static longitudinal stability at positive angles of attack but decrease at negative one. They also observed a reduction in induced drag and no change in wing profile as the wing approaches to ground. According to their investigation, the effect of the endplates, which are extended one-inch below and were parallel to the lower surface of the wing, was mentioned briefly. An endplate showed the effect of preventing the stagnated air on lower surface from flowing out around the wing tips and produced a substantial improvement in lift-drat ratio. On the other hand, the ground had no effect on the maximum lift of the plain wings but reduced the maximum lift coefficient of the wings equipped with split or slotted flaps.

Ahmed[5] and Hsiun and Chen[6] predicted the flow characteristics of NACA 4412 by both experiment and numerical. A sudden increase of the lift coefficient was observed as the ground was approaching because the stationary boundary was used. This increase was not happen in the real flight. Both investigations found the increase of the suction on the upper surface and increase of the pressure on the lower surface in two-dimensional flow. The pressure decrease on the lower surface offset the pressure on the lower surface at about 4 deg of angle of attack and the lift remained constant along the angle of attack. For zero-degree of the angle of attack($\alpha = 0^o$), the lift force was almost zero at height = 0.05 due to the strong suction effect on the lower surface and the laminar separation.

Many numerical and experimental studies were carried out to predict the aerodynamic characteristics of wing under the ground effect. However, much less study has been devoted to analyze the flow field around an endplate which has an aspect ratio (AR) of one. To the author's knowledge, the detailed aerodynamic analysis on the influence of endplate in WIG craft has not been reported. Therefore, in the present work, the influence of endplate on the aerodynamic characteristics of a rectangular wing in ground effect in viscous flow is studied numerically. Numerical analyses are performed by solving the Reynolds averaged Navier-Stokes (RANS) of turbulent flow and the aerodynamic characteristics (i.e., lift, lift-to-drag ratio, pressure distribution and static height stability) are compared for the case of with- and without endplate for various conditions such as angle of attack (α) and non-dimensional height (h/Chord).

II. NUMERICAL MODELING FOR WIG-AIRFOIL

A. Numerical Approaches

The physical configuration of endplate profile considered in this study is presented in Fig. 1. Air is taken as the fluid and is assumed to be steady and incompressible. The shape of endplate is three-dimensional one and the flow is turbulent. The fluid properties are taken to be constant and the effect of viscous dissipation is assumed to be negligibly small. Using the above-mentioned assumptions, the Reynolds-Averaged Navier -Stokes (RANS) equations for mass and momentum, which are written in a tensor notation, have to be solved.

$$\frac{\partial(\rho u_j)}{\partial x_j} = 0 \tag{1}$$

$$\frac{\partial(\rho u_i u_j)}{\partial x_j} = -\frac{\partial P}{\partial x_i} + \frac{\partial}{\partial x_j}\left[\mu\left(\frac{\partial u_i}{\partial x_j} + \frac{\partial u_j}{\partial u_i}\right) - \overline{\rho u_i' u_j'}\right] \tag{2}$$

The new term, $\overline{\rho u_i' u_j'}$, the Reynolds stress, must be modeled using a turbulence model in order to solve the RANS equations. In this study, the flow domain can be divided into two regions such as near wall and fully turbulent regions and then adopted a standard turbulent model [7] and low-Reynolds model, which is proposed by Norris and Reynold [8], respectively. According to this model, turbulent kinetic energy (k) and its dissipation rate (ε) are expressed in a tensor form as follows;
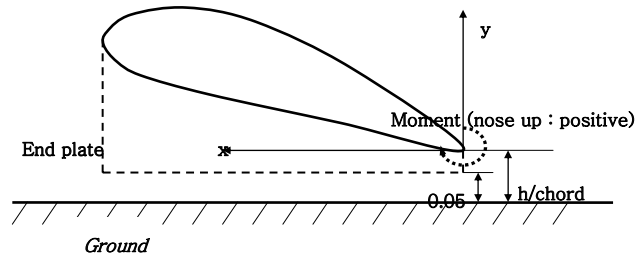

Fig. 1 Physical model of wing in ground effect

$$\frac{\partial}{\partial x_j}\left(\rho u_i k\right) = \frac{\partial}{\partial x_j}\left[\frac{\mu_t}{\sigma_k}\frac{\partial k}{\partial x_j}\right] + P_k - \rho\varepsilon \tag{3}$$

$$\varepsilon = \frac{k^{3/2}}{l_\varepsilon}\left(1 + \frac{C_\varepsilon}{\text{Re}_y}\right) \tag{4}$$

where i = 1,2 and 3 denote x, y, and z directions, respectively. The term P_k in Eq. (3) stands for the production term. The model constants and various functions used in the turbulent model are detailed in References [7,8].

The numerical simulations presented in this work are carried out by means of STAR-CD [9] which is one of general purpose commercial softwares. The pressure-velocity coupling phenomenon is resolved through the SIMPLE algorithm [10]. The moving boundary condition instead of the slip or non-slip boundary condition is employed for representing the exact flight conditions. The solutions are treated as converged ones when the sum of residual and the relative deviation of dependent variables between consecutive iterations are less than 10^{-5}.

B. Validation of CFD Model

The numerical results for modified Glenn Martine 21 airfoil at two different computational conditions are obtained by the present method and compared with the experimental data [3]. The airfoil is modified to provide a flat bottom wing from the 30% of the chord to the trailing edge. Computations are performed at $\alpha = 0^o$ with the aspect ratio of 1 and Reynolds number of 0.46×10^6 . Endplates did not attach in this case.
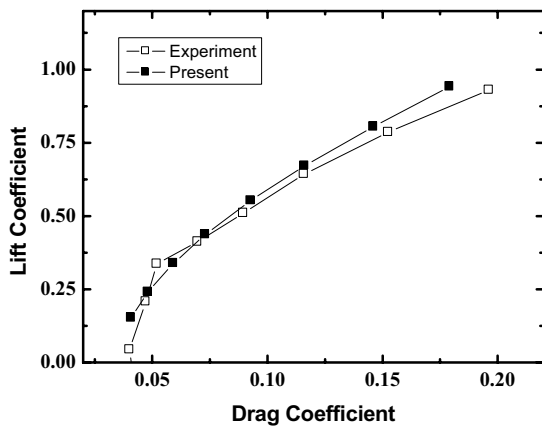
Fig. 2 shows the comparisons of lift coefficients and drag polar at **h/Chord** = 0.176 and 2 respectively and show good agreement with the experiments. The wings in Fig. 2(a)and (b) are sufficiently close to the ground and is in ground effect (IGE) while the wing in Fig. 2(c) and (d) is far away from the ground and is out of ground effect (OGE). The RNG k-ε model is used for prediction the turbulence flow and the near-wall flow is computed by using a wall function. Due to the geometric symmetry conditions of the model, only half of the model is simulated. Five-layers of the prism mesh are used to resolve the boundary layer on the wing surface and y_{max}^+ values are about 50 over the wing surface. The experiments were conducted by the image-wing method since this method did not present the boundary-layer problems between the wing and ground.
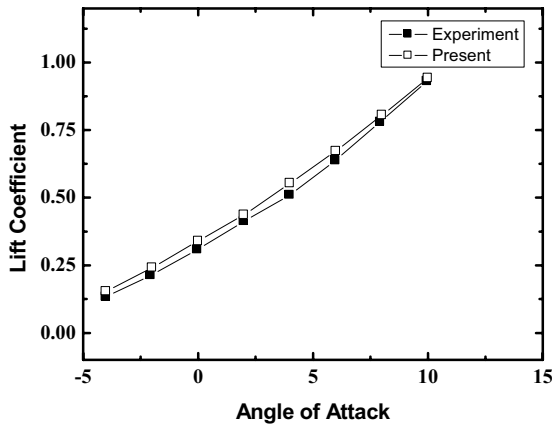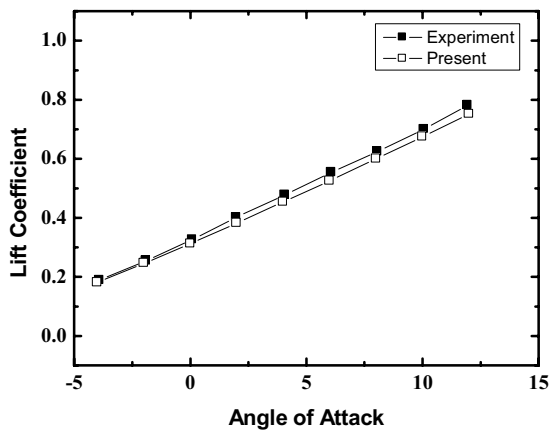
a) Lift coefficient at h/Chord=0.176
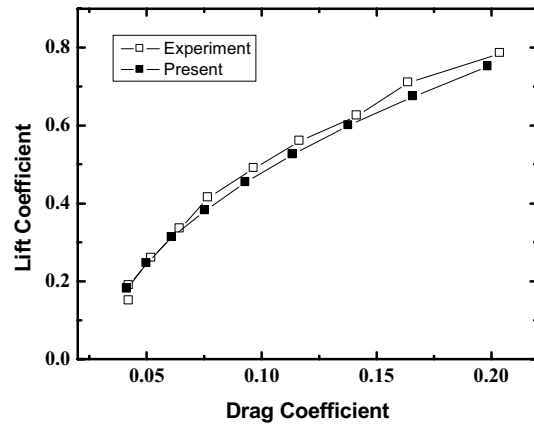
(b) Drag polar at h/Chord=0.176

(c) Lift coefficient at h/Chord=2.0

Fig. 2 Comparison of aerodynamic characteristics (continued)

(d) Drag polar at h/Chord=2.0

Fig. 2 Comparison of aerodynamic characteristics

the prism mesh are adopted to predict the accurate flow near the endplate and this grid system is shown in Fig. 3. In this study, the y^{+}_{max} values on the ground and on the wing surface are estimated less than 20 and 50 respectively. Non-dimensional height between the wing and ground is measured at the trailing edge and a nose-up pitching moment is positive as seen in Fig. 1. The bottom edge of an endplate is parallel to the ground surface. The distance between endplate and ground is remained constant irrespective of the height and angle of attack of airfoil in order to predict the aerodynamic performance for the cruise condition. Because of constant height of the endplate, the numerical calculation for with endplate is restricted at the minimum value of **h/chord** = 0.1 as shown in Fig. 1.

In order to explain the effect of endplate on the lift force according to the airfoil height (**h/chord**), the lift coefficients for various values of α (0 – 10 degree) are displayed in Fig. 4. Fig. 4(a) shows the results for without endplate and for the case of with-endplate is shown in Fig. 4(b). It is found that the proximity to the ground results in the increase of the lift force for all angles of attack. According to the wing profile, lift coefficients against heights are variable. For the symmetric airfoil without a camber or the airfoil with a moderate camber, low value of lift force is observed because of its
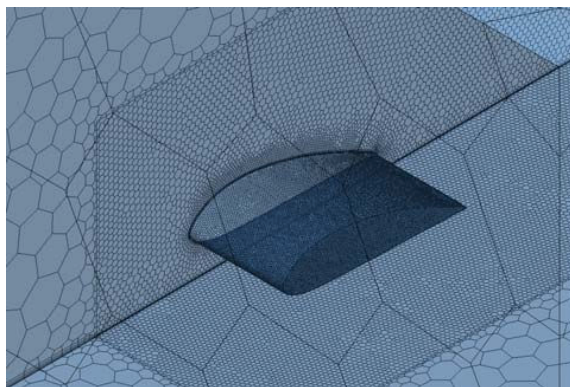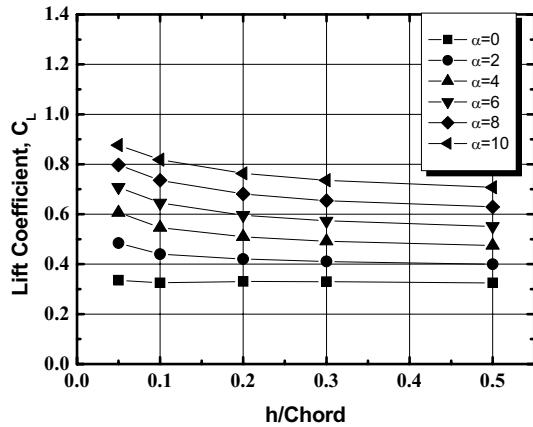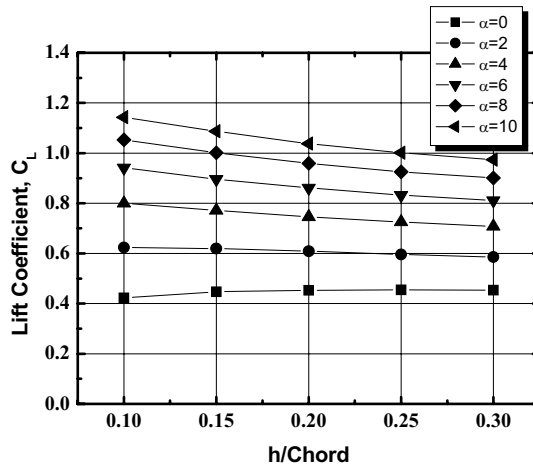
III. RESULTS AND DISCUSSION

The computational analysis for estimating the flow characteristics around the airfoil for three-dimensional turbulent flow is performed with the same grids and numerical schemes as discussed in the preceding chapter. Five-layers of

Fig. 3 Grid systems - polyhedral meshs

(a) without endplate
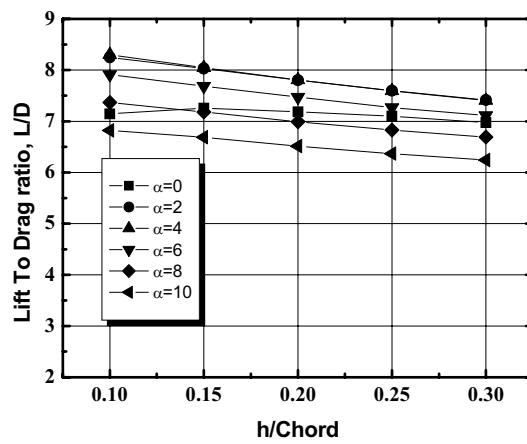

(a) without endplate

(b) with endplate

(b) with endplate

Fig. 4 Lift coefficient with respect to height

Fig. 5 Lift-to-drag ratio with respect to height

divergent-convergent passage as reported by Ref.s [6] and [11]. Ahmed and Sharma [12] showed the different results in their experiment with the symmetric airfoil of NACA0015. The difference is caused by both the blockage effect and the non-slip ground plate since the airfoil is almost contacted to the ground plate at **h/chord** = 0.1, which is measured from the ground to the trailing edge. The modified Glenn Martine 21 airfoil for the WIG craft used in this study has geometrical advantage and reduced the lift deep at low angles of attack somewhat. The same results as this study can be found in the study of Ahmed and Goonaratne [13]. They studied on the thick and low-aspect ratio airfoil with an endplate and showed that airfoils could provide lift augmentation when they were in the influence of the ground effect. They reported that the lift was increased as the angle of attack (i.e., cambered airfoil) increased for the NACA4415. In general, lift forces depends on three forces which are the suction on the upper surface, the divergent-convergent passage on the lower surface and the pressure augmentation on the lower surface. Hsiun at el. [6] also observed the increase of lift force as the height is decreased except for the very low height of **h/chord** < 0.25. The deep lift decrease came from the boundary layer due to the stationary ground in their study. For $\alpha = 0^o$ in Fig. 4(a), the lift is not changed except the very close to the ground but for $\alpha = 2 \sim 8^o$, the values of lift increase for **h/chord** < 0.3. At positive angles of attack, the WIG craft is therefore stable in height. Interestingly, the lift forces at $\alpha = 0^o$ is almost constant at **h/chord** > 0.1. Recant [14] also noted that the lift forces at $\alpha = 0^o$ were not shifted in his experiments of wings without high lift devices. On the other hand, it can be seen in Fig. 4 that the existence of endplate captures the increase of lift force compared with the case of without endplate for all conditions because of the high-pressure air under the airfoil. That is, the endplate brings on the increase in lift force at the same α and **h/chord**. However, the values of lift forces in Fig. 4(b) are decreased with reducing height at $\alpha = 0^o$. Interestingly, the slight decrease also can be seen in Fig. 4(a) at $\alpha = 0^o$ and **h/chord** =0.1. The decrease of lift forces comes form the thickness effect and leads to the instability of height.

Fig. 5 depicts the lift-to-drag ratio for the same conditions as Fig. 4. It can be easily seen in Fig. 5 that the airfoil with the endplate has larger value of the lift-to-drag ratios than that of without endplate. The lift-drag ratios in Fig. 5(a), which is the case of no endplate, is exponentially increased with decreasing height, while Fig. 5(b) shows that the lift-drag ratio is increased linearly for all α. Compared with two cases, the endplate
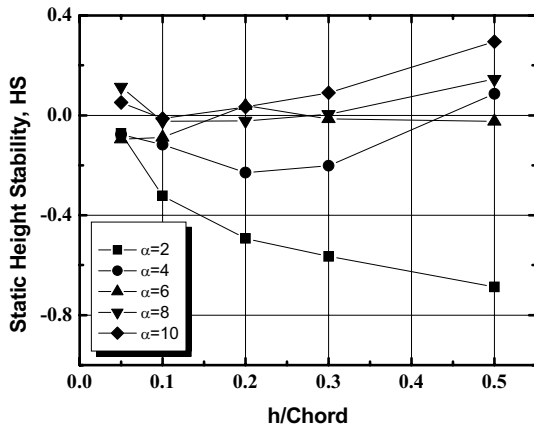
(a) without endplate
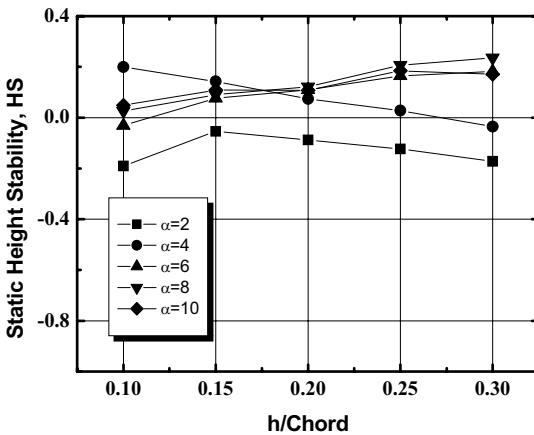
(b) with endplate

Fig. 6 Static height stability with respect to height

improves the lift-to-drag ratio due to the increasing in the air cushioning on the lower surface of the airfoil. However, the steep decreases of lift-drag ratio with the endplate are observed at $\alpha = 0^o$. This is caused by a decrease in lift as the ground height decreases as shown in Fig. 4(b). Carter [5] was carried out the experiments for the three different airfoils; Martin No.2, R.A.F 15 special and U.S.A. 27 and he found the same results at $\alpha = 0^o$. The largest value of lift-drag is observed at $\alpha = 2^o$ in Fig. 5 (a) and (b) and the lift-drag ratios are rapidly decreased at $\alpha > 2^o$.

Fig. 6 shows pictures of the static height stability (HS) proposed by Irodov [15]. The calculation of the static height stability condition includes the differentiations of lift coefficient and pitching moment coefficient against heights and angles of attack. To reduce the numerical errors, the differentiations are calculated from the interpolation function of lift coefficient and pitching moment instead of the direct numerical differentiation. Two different functions, second order polynomial for the lift coefficient and double exponential functions [14] for the moment coefficient, are employed and are:

$$C_L = C_{L0} + A_1\alpha + A_2\alpha^2 \tag{5}$$

$$C_M = C_{M0} + B_1 e^{h/Chord/t_1} + B_2 e^{h/Chord/t_2} \tag{6}$$

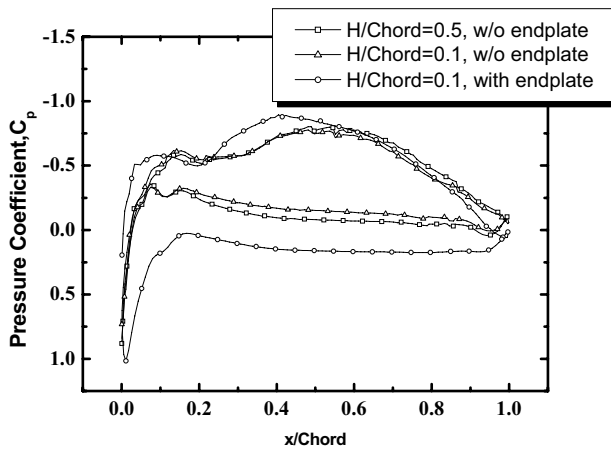where $C_{L0}, A_1, A_2, C_{M0}, B_1, t_1, B_2,$ and t_2 are independent variables for the curve regression.

$$HS = \frac{C_{M,\alpha}}{C_{L,\alpha}} - \frac{C_{M,h}}{C_{L,h}} = X_\alpha - X_h \leq 0 \tag{7}$$

where h and α in the moment coefficient and the lift coefficient represent the derivative of the height and the angle of attack respectively. The pitching moments are measured at a trailing edge. One might expect that the simplest condition for the static height stability is:
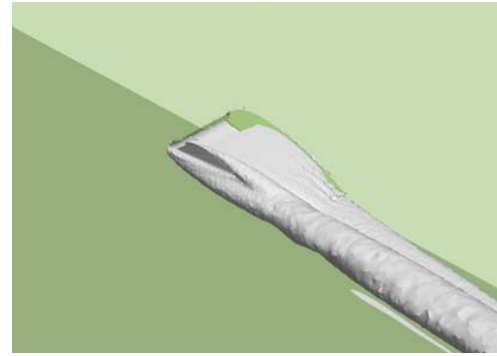
$$C_{L,h} < 0 \tag{8}$$

For the stability, when the increase of the height will indeed lead to the decrease of the lift, it apparently satisfies the stable condition. The fact that the moment coefficient changes due to the height is not, however, taken into account in Eq.(8). So the equation is only valid when the wing is in a trimmed condition; in other words C_M must be held constant. Eq.(7) takes into consideration of the actual conditions: lift and moment according to α and *h/chord*. As shown in Eq.(7), *HS* implies the distance between two neutral points, X_h for neutral point of heights (*h/chord*), and X_α for the neutral point of angles (α). The positive direction of the X , a distance measured from the trailing edge, is positive. Consequently, *HS* can be satisfied, if X_h is upstream of X_α. According to Fig. 6, it clearly shows that *HS* decreases with respect to *h/chord* at the low angles ($\alpha = 2^o$ and 4°) and increases at the high angles. Between two terms in the right-hand side of Eq.(7), these changes mainly come from X_h. Changes of the X_α against heights and angles of attack are moderate and linearly decrease as the height decreases. It implies that lift and pitching moment are linearly increase as angle of attack and the rate was not changed much except the ground is extremely close to the ground. The condition of *HS* for with endplate is only satisfied at $\alpha = 2^o$. The endplate is not favorable for *HS* since X_h for with endplate moves to around $x/Chord = 0.6$ while the X_h moves to at around $x/Chord = 0.7$ for without endplate. Compared Fig. 6(a) and (b), the deviation of *HS* for with endplate is, however, smaller than that for without endplate.

The pressure distributions on the wing surface in Fig. 7 show the details of the effect of the endplate. It is found that the considerable higher suction on the upper surface and the stagnation on the lower surface get enhanced due to the ground and the endplate. The reason can be said that some airs coming to the wing eventually stop on the lower surface and the rest flow over the upper surface which is divergent. On the other hand, the endplate prevents the flow exiting through the wing tip instead of the small gap at the trailing edge and consequently helps to argument the lift further. The lower pressure on the lower surface by stagnation is also observed in
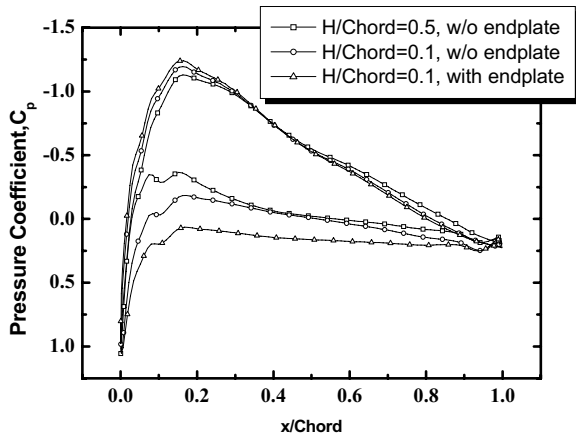
(a) z/Span=0.5

(b) z/Span=0.9

Fig. 7 Effect of the height and endplate on pressure coefficient
at $\alpha = 2^o$

(a) without endplate

(b) with endplate

Fig. 8 Effect of endplate on vorticity strength

studies on NACA 4412 [5, 6] but higher pressure on the upper surface is not. Modified Glenn Martine airfoil used in this study has divergence of the flow toward the upper surface and improves the lift further. In Fig. 7(b), the pressure distribution at around wing tip, triangles show the significantly lower pressures on the lower surface which have the same magnitude as that at mid-span. The endplate, which prevents air exit, keeps the high pressure on the lower surface until the wing tip. The wiggles on the upper surface imply the existence of the wing-tip vortex at that point. The iso-surfaces of strength of vorticity can visualize the wing-tip vortices as shown in Fig. 8. Two wing-tip vortices are generated from each side at the mid-chord, flow downstream and are growing. The strength of the vorticity for the endplate is much stronger and the center of the vortex is pushed outward from the wing tip. At $x / Chord = 1.0$, the two wing-tip vortices, which are not merged to one, are clearly observed in Fig. 8(b) and rapidly diminished along downstream. It is expected that the influence of the wing-tip vortex is considerably decreased as shown in Fig. 8(b).

IV. CONCLUSIONS

This work analyzed the aerodynamic characteristics around the airfoil (i.e., lift force, lift-to-drag ratio, pressure distribution and height stability) numerically in order to predict the effect of endplate. The endplate extending downward at the wing tip prevents escaping high-pressure air from under the wing and maximizes the ground effect while the drag force remains constant or slightly increases only. Unlike wings out of ground effect, the air is flowed to the wing tip and wing-tip vortex generated under the wing surface was pushed away from the wing tip. The airfoil under the ground effect increases the lift and decreases the drag and is favorable for the stability as it approaches the ground. The endplate also increases lift and lift-drag ratio further. The wing without an endplate at $\alpha = 6 \sim 10^o$ and with an endplate at $\alpha = 4 \sim 10^o$ do not satisfy the static height stability, HS. It is found that the stability is mainly affected by the X_h than X_α which linearly decrease as the height is decreased. Briefly, X_α moves forward while X_h moves backward at low α and moves forward at high α. Moving X_h downstream is favorable for the static stability. Interestingly, because of the suction at $\alpha = 0^o$, the lift-drag rapidly decreases for both the cases because of decrease in lift. On the other hand, the wing-tip vortex for the endplate is separated to two and has been diminished rapidly along

downstream. This may be one of the significant reasons of decreasing induced drag for the wing with endplate. The endplate captures the high-pressure air under the wing and increases the lift and lift-drag ratio further. From the visualization of computation results, two wing-tip vortices are generated from each surface of the wing tip and their strength are weak and diminished rapidly. The endplate can improve the aerodynamic characteristics and stability of the wings in ground effect, simultaneously.

REFERENCES

[1] http://www.se-technology.com.
[2] C. Wieselsberger, "Wing Resistance near the Ground," NACA TM No. 77, 1922.
[3] M.P. Fink and J.L. Lastinger, "Aerodynamic Characteristics of Low-Aspect-Ratio Wings in Close Proximity to the Ground," NASA TN D-926, 1961.
[4] A.W. Carter, "Effect of Ground Proximity on the Aerodynamic Characteristics of Aspect-Ratio-1 Airfoils with and without End Plate," NASA TN D-970, 1961.
[5] M. R. Ahmed, "Aerodynamics of a NACA4412 Airfoil in Ground Effect," AIAA Journal, Vol. 45, No. 1, 2007.
[6] C. Hsiun and C. Chen, "Aerodynamic Characteristics of a Two-Dimensional Airfoil with Ground Effect," J. of Aircraft, Vol. 33, No. 2, 1996.
[7] W. Rodi, Turbulence models and their applications in hydraulics-a state art of review, Book Publication of International Association for Hydraulic Research, Delft, Netherlands, 1984.
[8] L. H. Norris and W. C. Reynolds, *Turbulent Channel Flow with a Moving Wavy Boundary*, Report. FM-10, Department of Mechanical Engineering, Stanford University, CA, 1975.
[9] STAR-CD v4.00, Methodology, Computational Dynamics, Co., London. U. K, 2006.
[10] S.V. Patankar, *Numerical Heat Transfer and Fluid Flow*, McGraw-Hill Book Company, New York.
[11] Chang-Yeol Joh and Yang-Joon Kim, "Computational Aerodynamic Analysis of Airfoil for WIG (Wing-In-Ground-Effect) – Craft," JSAS, Vol. 32, No. 8 (Korean), 2004.
[12] M. R. Ahmed and S.D. Sharma, "An investigation on the aerodynamics of a symmetrical airfoil in ground effect," Experimental Thermal and Fluid Science, Vol. 29, pp. 633-647, 2005.
[13] N. A. Ahmed, and J. Goonaratne, "Lift Augmentation of a Low-Aspect-Ratio Thick Wing in Ground Effect," J. Aircraft, Vol. 39, No. 2, 2002.
[14] I.G. Recant, "Wing-Tunnel Investitation of Ground Effect on Wing with Flaps," NACA TN No. 705, 1939.
[15] R.D. Irodov, "Criteria of Longitudinal Stability of Ekranoplan," Ucheniye Zapiski TSAGI, Vol. 1, No. 4, 1970.